

# Fibre formation in the hydrostatic extrusion of linear polyethylene – sodium lignosulphonate blends

J. KUBÁT, J. -A. MÅNSON, M. RIGDAHL

*Chalmers University of Technology, Department of Polymeric Materials, S-412 96 Gothenburg, Sweden*

A blend consisting of equal amounts (by weight) of linear polyethylene and a technical grade of sodium lignosulphonate (a water soluble substance), was processed using hydrostatic extrusion with extrusion ratios varying from 5 to 20. The resulting extrudate contained thin (2 to 5  $\mu\text{m}$ ) fibres of the linear polyethylene in a matrix of the lignosulphonate. The fibres were basically continuous throughout the extrudate. Their stiffness was of the same order as that observed for pure hydrostatically extruded polyethylene. The fibre phase was easily isolated by dissolving the matrix material in water.

## 1. Introduction

During recent years an appreciable interest has been devoted to the production of strongly oriented high modulus semi-crystalline polymers, mainly linear polyethylene (LPE). The methods employed were, among others, tensile drawing [1, 2], shear crystallization from solution [3], capillary extrusion [4–6], high pressure injection moulding [7] and solid state extrusion. Ram extrusion [8, 9] and hydrostatic extrusion [10–12] were the two main lines of approach in the latter technique. A substantial amount of current knowledge about high modulus polyethylene has been summarized in two recent books [13, 14]. In some cases ultra-oriented linear polyethylene with a tensile modulus of 60 to 70 GPa has been obtained [11, 15].

In most cases, the methods for producing high modulus materials have been applied to homogeneous systems consisting of a single polymer. Solid state co-extrusion of sandwiched or concentric structures has been developed by Porter and co-workers [16, 17]; the structure studied normally consisted of two polyethylene types. According to the available literature, little interest appears to have been devoted to hydrostatic extrusion of heterogeneous structures, such as filled or reinforced polymers, polymer alloys, or polymers containing low molecular weight components.

One exception to this is the investigation by Maruyama *et al.* [18] concerning the properties of ram-extruded blends of linear polyethylene and *n*-paraffin and the related processing technique. Another example, although not related to the semi-crystalline polyolefins, is the study of hydrostatic extrusion of high-impact polystyrene by Ariyama *et al.* [19]. The production of oriented films and fibres of polyethylene–polypropylene blends from solution reported by Coombes *et al.* [20] could also be mentioned in this connection.

In this paper the hydrostatic extrusion of a composite material consisting of 50 wt% linear polyethylene and 50 wt% of a technical grade of sodium lignosulphonate, a water soluble substance, is reported. The primary intention was to study the formation of polyethylene fibres in this system, from which the fibres can be easily recovered by water extraction. The thin, basically continuous fibres formed by the polyethylene phase had a tensile modulus of the same order as that obtained with the pure polymer extruded using the same technique. The extrusion ratio was varied between 5 and 20; the extrusion temperature was 112 and 125°C. It was noted that the addition of lignosulphonate allowed lower extrusion temperatures and pressures to be used than for the pure polymer at the same extrusion rate. With the equipment used,

extrusion rates of  $500 \text{ mm min}^{-1}$  were easily obtained at temperatures around  $112^\circ \text{C}$ , at an extrusion ratio of 10 and with a pressure of about 40 MPa.

The formation of fibres in, e.g., capillary extrusion of polymer blends, is well known [21, 22], although it has not been discussed in connection with high modulus systems. It has been proposed that if fibres are formed, it is the more viscous component which constitutes these fibres [22]. This appears to be in agreement with the results obtained in the present work.

## 2. Experimental procedure

### 2.1. Materials

The linear polyethylene (LPE) grade used in this work was Rigidex 50, supplied by BP Chemicals Int. Ltd. The average molecular weights were reported as  $\bar{M}_w = 101\,450$  and  $\bar{M}_n = 6\,180$  [11]. The melt flow index was 6.0 g per 10 min (BS 2782 Method 10S C) and the density  $0.962 \text{ g cm}^{-3}$ .

The sodium lignosulphonate used was Wanin S, supplied by Holmens Bruk, Vargön, Sweden. As it was obtained by evaporation of sulphite spent liquor, it contained appreciable amounts of sugars and inorganic salts. The composition is given in Table I.

### 2.2. Preparation of the billets for hydrostatic extrusion

A blend of 50 wt % LPE and 50 wt % Wanin S was homogenized in a mixing extruder (Co-Kneter, Buss AG,  $L/D = 11$ ,  $D = 46 \text{ mm}$ ) at approximately  $180^\circ \text{C}$ . The temperature was kept relatively low in order to prevent thermal degradation of the lignosulphonate. The homogenized mixture was granulated, whereafter it was injection moulded on a conventional machine (Arburg 221 E/170 R) into cylindrical rods with the length 120 mm and the diameter varying from 5.6 to 11.2 mm. The injection pressure was 150 MPa and mould temperature  $40^\circ \text{C}$ . The holding time was extended to

about 90 sec to avoid air entrapments. The end sections of the mouldings were cut off and the remaining billet (with a length of approximately 110 mm) was used for the hydrostatic extrusion.

### 2.3. Hydrostatic extrusion

The equipment used for the hydrostatic extrusion is shown in Fig. 1. The pressure is developed by a piston, and the extrudate is forced through the die as indicated in Fig. 1. The semi-angle of the die was  $15^\circ$ . Castor oil (pharmaceutical grade) was used as the pressure medium. The area reduction (extrusion ratio,  $R_N$ ) varied between 5 and 20 depending on the diameter of the billet; the bore diameter was always 2.5 mm.

Before extrusion the billets were covered with a thin plastic film (EVA), to prevent possible stress cracking due to contact with the castor oil. Two extrusion temperatures were used, 112 and  $125^\circ \text{C}$ , and the extrusion rate was approximately  $35 \text{ mm min}^{-1}$ . Under these conditions the hydrostatic pressure varied between 20 and 40 MPa, depending on the extrusion ratio, at an extrusion temperature of  $125^\circ \text{C}$ , and between 45 and 130 MPa at  $112^\circ \text{C}$ , see Fig. 2.

In a series of experiments the effect of the extrusion rate which was up to  $500 \text{ mm min}^{-1}$  at  $112^\circ \text{C}$  was studied. The maximum hydrostatic pressure was approximately 40 MPa.

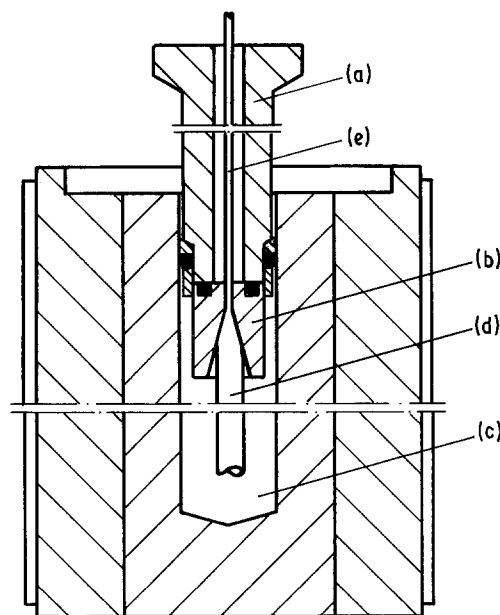


Figure 1 Schematic drawing of the device for hydrostatic extrusion showing (a) Piston, (b) Die, (c) Pressure medium (castor oil), (d) Billet (pre-extrudate), (e) Extrudate.

TABLE I. Typical composition of Wanin S

Component	Content (wt %)
High molecular weight sodium lignosulphonates	60
Salts of low molecular weight organic acids	10
Reducing matter calculated as glucose	25
Other substances	5

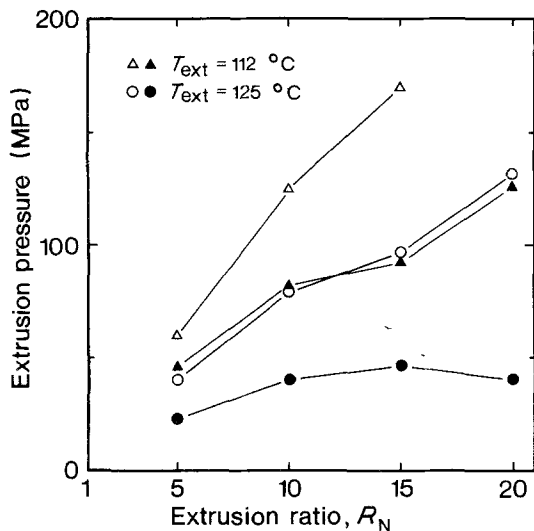


Figure 2 Extrusion pressure against extrusion ratio for LPE and LPE–Wanin S with an extrusion temperature of 112° C and 125° C. Closed symbols refer to LPE–Wanin S and open symbols refer to LPE.

For comparison, pure LPE (Rigidex 50) was extruded using the same technique. To obtain the same extrusion rate as with the composites (35 mm min<sup>-1</sup>) the hydrostatic pressure had to be raised, see Fig. 2.

The fibres were extracted from the extrudate by dissolving the Wanin S matrix in water at room temperature, a process completed in a few minutes.

## 2.4. Testing

### 2.4.1. Tensile testing

The stress–strain properties in the extrusion direction were determined at room temperature (20 ± 0.5° C) with an Instron tensile testing machine (model 1193). The strain rate was 3.3 × 10<sup>-4</sup> sec<sup>-1</sup> and all measurements were performed using an extensometer (gauge length 25 mm). The secant modulus was evaluated at 0.1% strain. The stress–strain measurements were performed on the extrudate only; attempts to determine the mechanical behaviour of individual fibres were unsuccessful.

### 2.4.2. Flow curves

The flow curves for the LPE–Wanin S melts were determined at 180° C using a capillary viscometer (Instron machine, model 3211).

### 2.4.3. Shrinkage

The shrinkage,  $S$ , of the polyethylene fibres, measured in the temperature interval 131 to 145 (± 0.2°) C, was calculated as

$$S = \frac{L_0 - L}{L_0}, \quad (1)$$

where  $L_0$  and  $L$  are the length of the fibres before and after the heat treatment, respectively. The fibres were isolated from the Wanin S matrix by water extraction. The shrinkage was determined after 10 min immersion in silicone fluid of the corresponding temperature.

### 2.4.4. Thermal analysis

The melting point,  $T_m$ , and heat of fusion,  $\Delta H_f$ , of the fibres were determined with a differential thermal analysis device (Mettler TC 2000). The heating rate was 5° C min<sup>-1</sup> and the  $T_m$  values obtained were compensated for the influence of the heating rate.

### 2.4.5. Wide angle X-ray scattering (WAXS)

The WAXS patterns were obtained at room temperature using a pin-hole camera and nickel-filtered CuK $\alpha$ -radiation. The specimens were mounted with their flow direction perpendicular to the incident X-ray beam.

### 2.4.6. Scanning electron microscopy (SEM)

Scanning electron micrographs of the LPE-fibres were obtained with a JEOL JSM-35 machine.

## 3. Results

As already mentioned, extrusion of the blends yields a composite consisting of LPE fibres embedded in the Wanin S matrix. It should be stressed that LPE fibres are present in the composite both before and after the hydrostatic extrusion although, as will be described later, the fibres are significantly shorter and less uniform prior to the hydrostatic process. The SEM reproduced in Fig. 3 clearly shows the fibrous character of the LPE-phase (after hydrostatic extrusion). In preparing this photograph the matrix material was partly removed by a short water treatment, to give a better picture of the structure.

### 3.1. Tensile properties

In Fig. 4 the tensile modulus in the extrusion direction is shown for pure LPE against the extrusion ratio,  $R_N$ , for the two temperatures used. The improvement in stiffness with increasing  $R_N$  value is in agreement with results reported earlier using similar techniques (capillary and hydrostatic extrusion) [6, 10]. It may be remarked

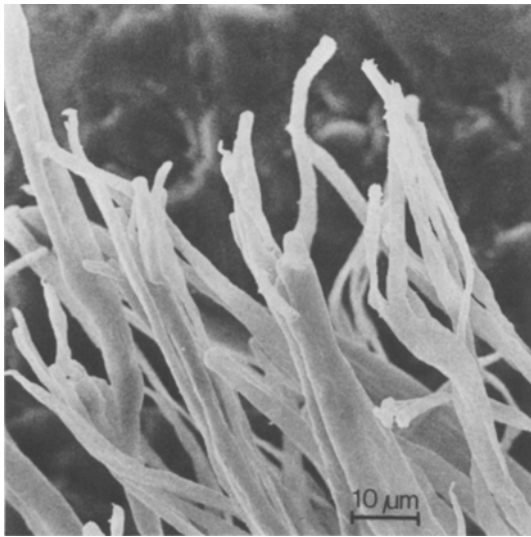


Figure 3 Scanning electron micrograph of the LPE fibres in the extrudate. The Wanin S phase has been removed by a short water treatment.

that in later works on hydrostatic extrusion Gibson and Ward have reported even higher values of the modulus at the same extrusion ratio [11].

Stress-strain curves for pure LPE and a LPE-Wanin S composite, hydrostatically extruded at 112°C with an extrusion ratio of 10, are shown in Fig. 5. In Fig. 5 the tensile behaviour of the composite prior to the hydrostatic extrusion is also given. In agreement with earlier reports [10 to 12], the hydrostatic extrusion significantly

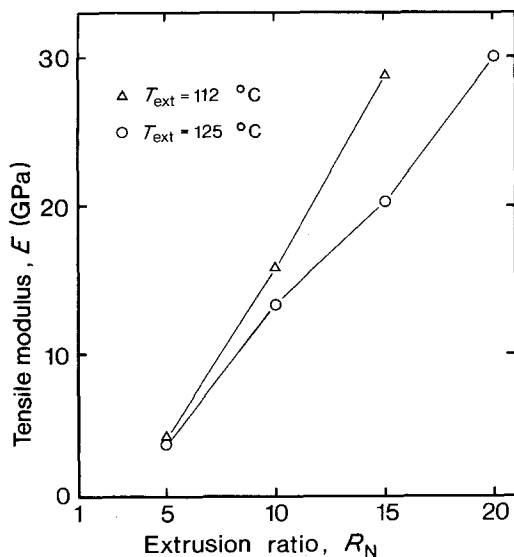


Figure 4 Tensile modulus,  $E$ , against the extrusion ratio,  $R_N$ , for pure LPE.

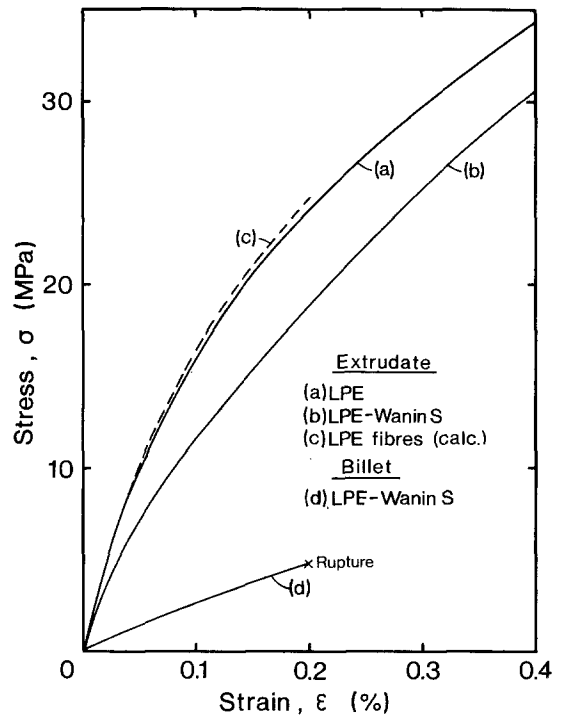


Figure 5 Stress-strain curves for (a) LPE and (b) LPE-Wanin S extrudates. Curve c corresponds to the stress-strain curve for the LPE fibres calculated from Equation 2, and Curve d is the experimental stress-strain curve for LPE-Wanin S billet (before the hydrostatic extrusion).

improves the mechanical properties of the parent material. It may be noted that prior to the extrusion the composite has a very low ductility (elongation at rupture, 0.2%), while afterwards it behaves similarly to the pure LPE up to 1.5% strain (which is the maximum strain used in this work, not shown in Fig. 5).

It was found difficult to perform stress-strain measurements on individual fibres isolated from the extrudate. The mechanical behaviour of the fibres had therefore to be determined in an indirect way. Several possibilities can be considered for this. The method adopted here can serve as a general guideline.

Assuming that a simple parallel model (constant strain model) is valid, the tensile modulus of the hydrostatically extruded LPE-fibres,  $E_F$ , in the composite is given by

$$E_F = \left( E_C - W_M \frac{\rho_C}{\rho_M} E_M \right) \frac{\rho_F}{\rho_C W_F}, \quad (2)$$

where  $E_F$  denotes the tensile modulus of LPE fibres,  $E_C$  is the modulus of the hydrostatically extruded composite,  $E_M$  is the modulus of Wanin

S,  $W_F$  is the weight-fraction of LPE (0.5),  $W_M$  the weight-fraction of Wanin S (0.5), and  $\rho_C, \rho_M, \rho_F$  are the densities of the composite ( $1.18 \text{ g cm}^{-3}$ ), Wanin S ( $1.53 \text{ g cm}^{-3}$ ) and LPE ( $0.962 \text{ g cm}^{-3}$ ), respectively.

The tensile modulus of Wanin S was estimated, using the parallel model, from the stiffness of the composite prior to hydrostatic extrusion and assuming that this extrusion did not markedly influence its mechanical properties. In this way an  $E_M$  value of 6.0 GPa was obtained. For the composite shown in Fig. 5, Equation 2 then yields a tensile modulus of 15 GPa for the individual fibres.

Using the same model as above the stress-strain curves for the LPE fibres in the composite (extrusion ratio 10 and extrusion temperature  $112^\circ \text{C}$ ) can be constructed. As is shown in Fig. 5, the tensile properties of the fibres are practically the same as those registered for the pure material processed under similar conditions. This indicates that the final structure of the thin polyethylene fibres is similar to that of the pure hydrostatically extruded LPE, at least at this extrusion temperature and ratio.

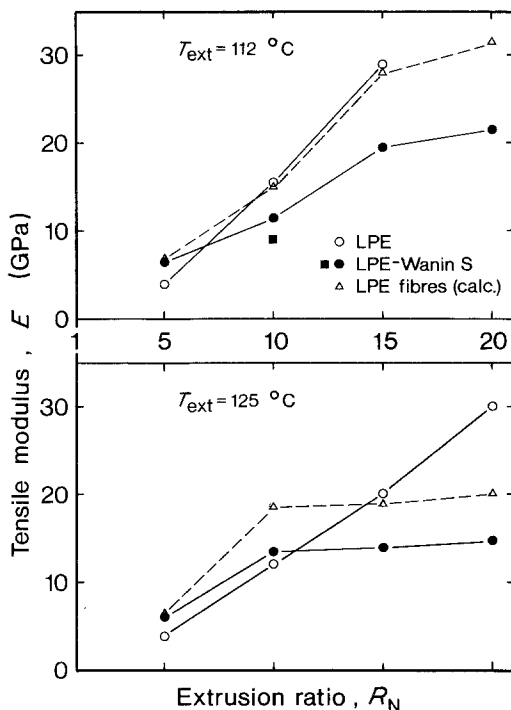


Figure 6 Tensile modulus,  $E$ , against extrusion ratio,  $R_N$ , for (○) LPE, (●) LPE-Wanin S and (△) LPE fibres, calculated from Equation 2. The LPE-Wanin S composite extruded with a rate of  $500 \text{ mm min}^{-1}$  is denoted with (■).

In Fig. 6 the tensile modulus is shown as a function of the extrusion ratio for the pure LPE and the composite. The modulus of the individual fibres in the composites, also shown in Fig. 6, is calculated according to Equation 2. For the specimen extruded at  $112^\circ \text{C}$  the modulus of the fibres increases from approximately 7 GPa (extrusion ratio 5) to approximately 32 GPa (extrusion ratio 20). Above an extrusion ratio of 15 there appears to be a tendency for the modulus to level off while at lower extrusion ratios (10 and less) the modulus of the fibres is close to that of the pure polyethylene. For specimens extruded at  $125^\circ \text{C}$  (Fig. 6) the calculated fibre modulus is higher than for the pure LPE at lower extrusion ratios, while above  $R_N = 10$  the modulus is approximately constant.

In Fig. 6 the tensile modulus for a composite extruded at  $500 \text{ mm min}^{-1}$  is given. Evidently, an increase in extrusion rate from 35 to  $500 \text{ mm min}^{-1}$  results in a reduction of the stiffness. This is probably due to the increased heat dissipation.

### 3.2. Flow curves

Fig. 7 shows the shear stress,  $\tau$ , against the shear rate  $\dot{\gamma}$  for LPE-Wanin S melts, containing various amounts of the lignosulphonate. The flow curves have been corrected according to Rabinowitsch. An increase in the Wanin S content results in a downward shift of the flow curves. The experimental results are fitted to a power-law relation, i.e.

$$\tau = K\dot{\gamma}^n, \quad (3)$$

and the influence of the composition of the blends on the constant  $K$  and  $n$  are shown in Table II. Evidently, the amount of Wanin S does not influ-

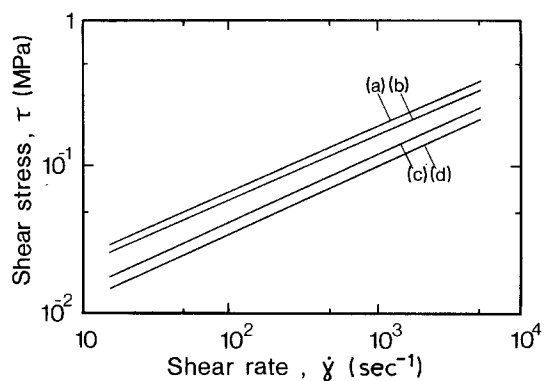


Figure 7 Flow curves for LPE containing (a) 0 wt%, (b) 10 wt%, (c) 30 wt%, (d) 50 wt% Wanin S at a temperature of  $180^\circ \text{C}$ .

TABLE II. Constants of the power law for the LPE-Wanin S melts

Material	$K$ (MPa sec <sup><i>n</i></sup> )	$n$
LPE	$9.1 \times 10^3$	0.44
90 wt % LPE-10 wt % Wanin S	$8.1 \times 10^3$	0.44
70 wt % LPE-30 wt % Wanin S	$5.2 \times 10^3$	0.45
50 wt % LPE-50 wt % Wanin S	$4.4 \times 10^3$	0.45

ence the value of the exponent  $n$ , while the consistency,  $K$ , decreases with increasing Wanin S content.

### 3.3. Shrinkage

The amount of shrinkage plotted against temperature is shown in Fig. 8 for the individual fibres at different extrusion ratios. In general, fibres obtained with lower extrusion ratios start to shrink at lower temperatures, i.e., higher extrusion ratios result in a more temperature-stable structure. Increasing the temperature above 137°C does not have any significant influence on the amount of shrinkage. The final shrinkage level is about 75% for the fibres, independent of the extrusion temperature.

Some experiments on the shrinkage of the fibres at lower temperatures (down to 90°C) were also performed. The observed behaviour is in general similar to that reported by Gibson and Ward [13], i.e., a slow increase in shrinkage up to 120°C, fol-

lowed by a substantial contraction at higher temperatures.

### 3.4. Thermal analysis

The melting points,  $T_m$ , of the polyethylene fibres in the composites and the pure material are shown in Fig. 9 plotted against the extrusion ratio. As expected, hydrostatic extrusion produces a shift in  $T_m$  to higher temperatures. Similar effects have been reported by others [8, 10]. For fibres produced at 112°C the melting point increases from about 132 to 139°C at an extrusion ratio of 20. Above  $R_N = 10$ , the increase in  $T_m$  is, however, rather limited. For fibres extruded at 125°C, there is a decrease in melting point for the highest extrusion ratio used here. Also for pure LPE, it is found that the rate of increase in  $T_m$  decreases at higher extrusion ratios [6].

Similar behaviour is observed when the crystallinity of the fibres is plotted against the extrusion ratio, Fig. 10. Here the crystallinity is estimated on the basis of the specific heat, with  $\Delta H_f = 290 \text{ J g}^{-1}$  for completely crystalline polyethylene [23]. At an extrusion temperature of 125°C the crystallinity attains a maximum (87%) at an extrusion ratio of 15 and then decreases, while for the fibres extruded at 112°C the crystallinity increases up to above 90% at the higher ratios used. Prior to the hydrostatic extrusion the crystallinity was 72%.

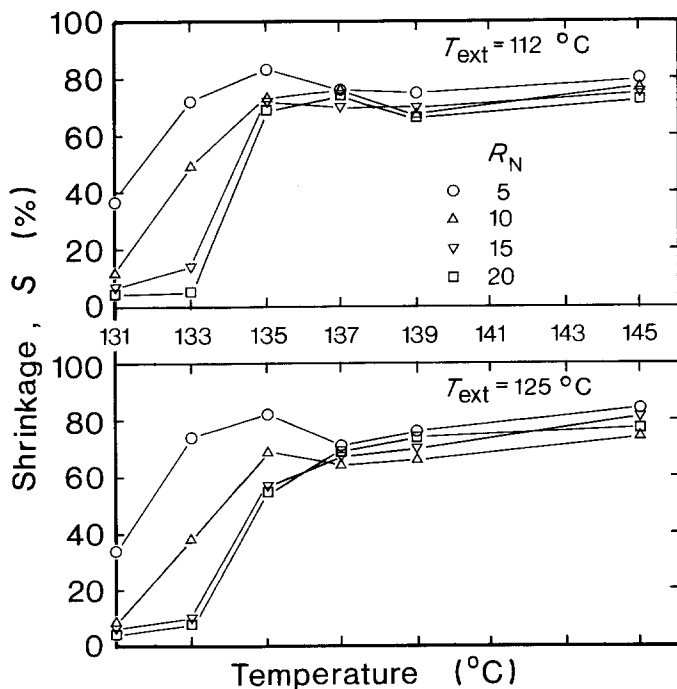


Figure 8 Shrinkage,  $S$ , of the LPE-fibres, extruded with different extrusion ratios, against temperature.

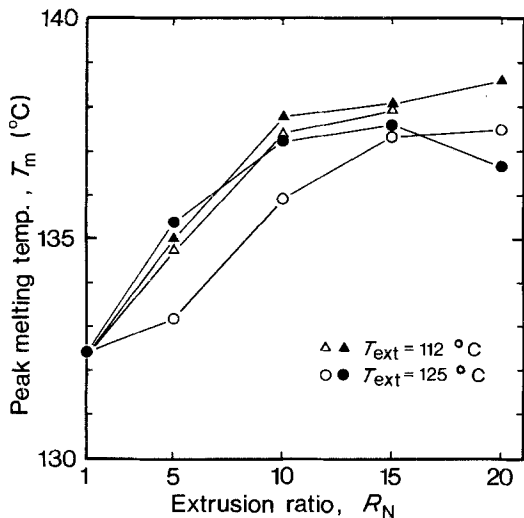


Figure 9 Peak melting temperature,  $T_m$ , against extrusion ratio for the pure LPE (unfilled symbols) and the LPE fibres (filled symbols) in the composite.

The crystallinity of the pure LPE was lower than that of the fibres but on the other hand it did increase monotonically with the extrusion temperature.

It can be noted that the  $T_m$ -values and crystallinities of the fibres were obtained from measurements on the composite, not on isolated fibres. In some cases, the Wanin S phase was removed by a

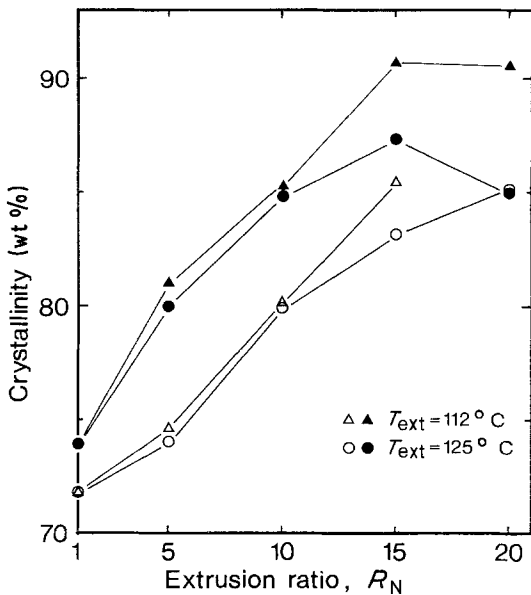


Figure 10 Crystallinity against extrusion ratio for LPE (unfilled symbols) and the LPE fibres (filled symbols) in the composite with extrusion temperatures of  $112^\circ\text{C}$  and  $125^\circ\text{C}$ .

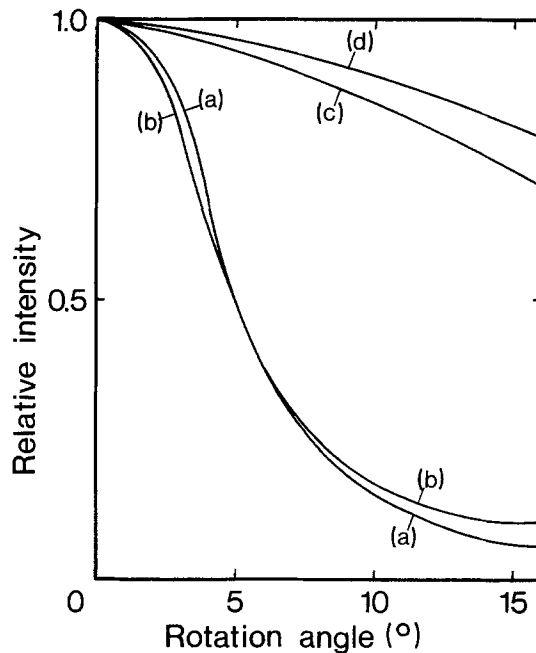


Figure 11 [110] azimuths for (a) LPE extrudate, (b) LPE fibres after hydrostatic extrusion, (c) LPE billet and (d) LPE fibres before hydrostatic extrusion.

water treatment. This did not appreciably affect the  $T_m$  and  $\Delta H_f$  values reported above.

### 3.5. Wide angle X-ray scattering

In Fig. 11, the [110] azimuths obtained from the X-ray diffraction patterns of the extrudates before and after the hydrostatic extrusion are shown, for both pure LPE and the composite. Prior to the hydrostatic extrusion no significant crystal orientation is present in either the pure LPE or the composite, while the diffraction patterns for the hydrostatic extrudates are typical for oriented polyethylene. The removal of the matrix material did not have any influence on the diffraction pattern of the fibres.

Apart from the well-known [110] and [200] reflections, there is also a faint diffraction ring in the hydrostatically extruded material (both pure LPE and composite) corresponding to a monoclinic structure. The corresponding spacing of the crystal planes was 0.455 nm, which is in good agreement with the results obtained by Porter and co-workers when producing high modulus polyethylene with capillary extrusion [24].

### 3.6. Scanning electron microscopy

From the scanning electron micrographs shown in Fig. 12 it is obvious that the composites consist of

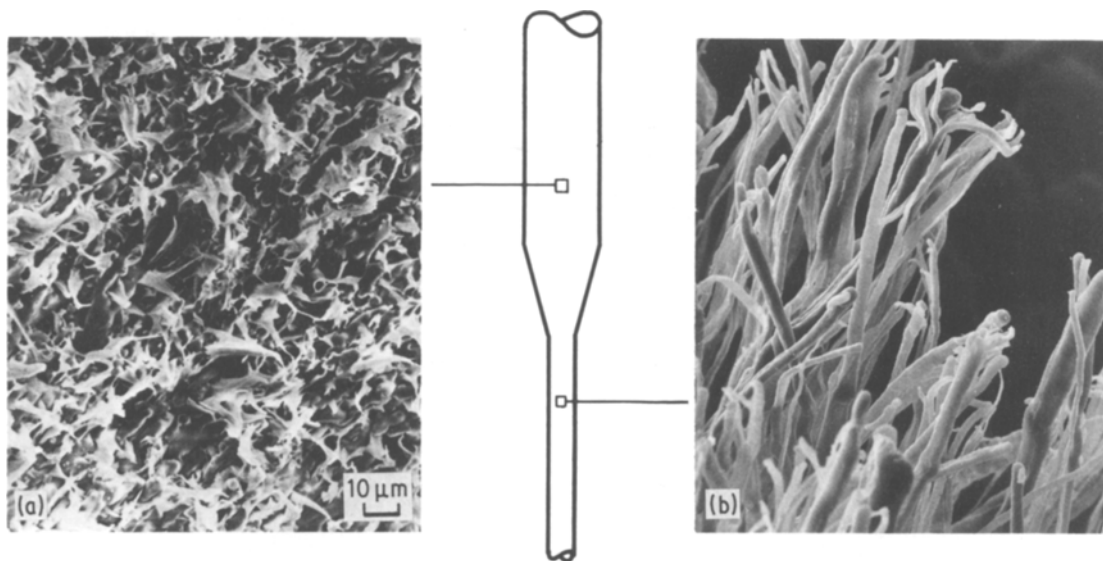


Figure 12 Scanning electron micrographs of the LPE fibres in the composite (a) before and (b) after hydrostatic extrusion.

LPE fibres immersed in a matrix of the lignosulphonate even prior to the hydrostatic extrusion. However, those LPE fibres are rather short, and non-uniform, which is partly reflected in the low ductility of the specimens, see above. The area and the shape of the fibre cross-section in the moulded billet prior to extrusion depends on distance from the surface. In general the cross-section of the fibres decreases in area and acquires a more circular shape with increasing distance from the surface. Near the surface, the fibres had an almost rectangular cross-section.

The fibres in the hydrostatic extrudate are more homogeneous with regard to the shape of the cross-section (mainly circular) and the fibre diameter. Typical fibres are also shown in Fig. 12. In contrast to the fibres in the pre-extrudate, the fibres in the hydrostatically extruded composites are visually continuous. The fibre diameter is of the order of 2 to 5  $\mu\text{m}$ .

#### 4. Discussion

The results presented in this paper demonstrate the basic feasibility of fibre production by hydrostatic extrusion of a heterogeneous polymer system. With regard to the properties of the fibres obtained by this process, it can be noted that their properties are similar to those of the solid extrudate of pure LPE. This applied to both mechanical properties such as the modulus, and certain thermal parameters, such as the melting temperature and

the shrinkage behaviour. The Wanin S phase appears here to have no influence on the properties of the LPE fibres, its role being merely the initiation and enhancement of fibre formation by initial phase separation. Wanin S was chosen simply because of its possible technical use as a relatively cheap additive easily removed from the extruded fibre mass by dissolving in water. Similar results would have probably been obtained with a number of other water soluble substances having similar physical characteristics and being largely incompatible with the polymer phase. With regard to the characteristics of the lignosulphonate used, its lubricating action, see Table II, may be noted as an important factor when higher extrusion rates are contemplated.

It has not been the aim of this paper to focus on the structure of the fibres obtained. The similarity between their properties and those of the solid LPE-extrudate seems to indicate that the structure may be largely similar. For extrusion ratios higher than about 10, Gibson *et al.* [12] proposed a structure consisting of stacks of crystallites with the *c*-axis mainly oriented in the extrusion direction and with intercrystalline bridges oriented in the same direction.

With regard to the influence of the extrusion temperature, there was, in general, a decrease in the modulus, in  $T_m$  and in the crystallinity at higher extrusion ratios at an extrusion temperature of 125°C. From Fig. 2 it is further noted that the



required extrusion pressure decreases when an extrusion ratio of 20 is used. These results indicate that the heat dissipated during the hydrostatic extrusion retards the improvement in physical properties, at least at higher extrusion temperatures and ratios. This and related problems have been discussed in detail by Gibson and Ward [11].

The shrinkage behaviour (Fig. 8) may appear somewhat puzzling since the fibres obtained at  $R_N = 5$  actually shrink more than those produced at  $R_N = 20$ , around 133°C. Considering the level of orientation of these fibres, the reverse behaviour is perhaps more natural. However, the shrinkage of the fibres obtained at higher extrusion ratios is to a certain extent retarded by the more thermally stable structure of this material. This results in a more dimension-stable material in this temperature region.

As already mentioned, fibre formation was also observed in the billets produced by normal extrusion, see Fig. 12. This effect, especially with regard to the dependence of the fibre morphology on the processing conditions, has been studied separately and the results will be published elsewhere [25]. The possibility of obtaining highly fibrillated structures appears promising as a means of producing synthetic wood pulp. However, the strength of such fibres, as produced under conditions of normal extrusion, is limited. It was against this background that the potential of hydrostatic extrusion as a means of improving the mechanical characteristics of such fibres was considered.

### Acknowledgement

The support of the Swedish Board for Technical Development in financing this work is gratefully acknowledged.

### References

1. G. CAPPACIO and I. M. WARD, *Polymer Eng. Sci.* **15** (1975) 219.
2. P. J. BARHAM and A. KELLER, *J. Mater. Sci.* **11** (1976) 27.
3. A. ZWIJNENBURG and A. J. PENNING, *Coll. Polymer Sci.* **254** (1976) 868.
4. R. S. PORTER, J. H. SOUTHERN and N. WEEKS, *Polymer Eng. Sci.* **15** (1975) 213.
5. S. KOJIMA and R. S. PORTER, *J. Polymer Sci., Polymer Phys. Ed.* **16** (1975) 1729.
6. W. T. MEAD and R. S. PORTER, *Int. J. Polymeric Mater.* **7** (1979) 29.
7. K. DJURNER, J. KUBÁT and M. RIGDAHL, *Polymer* **18** (1977) 1068.
8. K. IMADA, T. YAMAMOTO, K. SHIGEMATSU and M. TAKAYANAGI, *J. Mater. Sci.* **6** (1971) 537.
9. K. IMADA and M. TAKAYANAGI, *Int. J. Polymeric Mater.* **2** (1973) 89.
10. A. G. GIBSON, I. M. WARD, B. N. COTE and B. PARSONS, *J. Mater. Sci.* **9** (1974) 1193.
11. A. G. GIBSON and I. M. WARD, *J. Polymer Sci. Polymer Phys. Ed.* **16** (1978) 2015.
12. A. G. GIBSON, G. R. DAVIES and I. M. WARD, *Polymer* **19** (1978) 683.
13. A. CIFERRI and I. M. WARD (EDS), "Ultra-high Modulus Polymers" (Applied Science Publishers Ltd., Barking, England, 1979).
14. R. L. MILLER (ED) "Flow-induced Crystallization in Polymer Systems" Midland Macromolecular Monographs, Vol. 6, (Gordon and Breach, New York, USA, 1979).
15. N. G. PERKINS, N. J. CAPIATI and R. S. PORTER, *Polymer Eng. Sci.* **16** (1976) 200.
16. A. E. ZACHARIADES, R. BALL and R. S. PORTER, *J. Mater. Sci.* **13** (1978) 2671.
17. W. T. MEAD and R. S. PORTER, *J. Appl. Polymer Sci.* **22** (1978) 3249.
18. S. MARUYAMA, K. IMADA and M. TAKAYANAGI, *Int. J. Polymeric Mater.* **2** (1973) 105.
19. T. ARIYAMA, T. NAKAYAMA and N. INOUE, *Plastics Industry News*, June (1980) 85.
20. A. COOMBES, C. G. CANNON and A. KELLER, *J. Polymer Sci. Polymer Phys. Ed.*, **17** (1979) 1957.
21. M. V. TSEBRENKO, A. V. YUDIN, T. I. ABLAZOVA and G. V. VINOGRADOV, *Polymer* **17** (1976) 831.
22. N. ALLE and J. LYNGBAAE-JÖRGENSEN, *Rheol. Acta* **19** (1980) 104.
23. J. H. SOUTHERN and R. S. PORTER, *J. Appl. Polymer Sci.* **14** (1970) 2305.
24. C. R. DESPER, J. H. SOUTHERN, R. D. ULRICH and R. S. PORTER, *J. Appl. Phys.* **41** (1970) 4284.
25. P. ALBIHN and J. KUBÁT, unpublished work.

Received 19 March  
and accepted 18 August 1981